

# Magnetized accretion disks around Kerr black holes with scalar hair

Sergio Gimeno-Soler<sup>1</sup>, José A. Font<sup>1,2</sup>, Carlos Herdeiro<sup>3</sup>, Eugen Radu<sup>3</sup>

<sup>1</sup> Departamento de Astronomía y Astrofísica, Universitat de València, Dr. Moliner 50, 46100, Burjassot (València), Spain.  
 e-mail: sergio.gimeno@uv.es

<sup>2</sup> Observatori Astronòmic, Universitat de València, C/ Catedràtic José Beltrán 2, 46980, Paterna (València), Spain.  
 e-mail: j.antonio.font@uv.es

<sup>3</sup> Departamento de Física da Universidade de Aveiro and Centre for Research and Development in Mathematics and Applications (CIDMA), Campus de Santiago, 3810-183 Aveiro, Portugal

## ABSTRACT

We present a method to build magnetized constant angular momentum disks around Kerr black holes with scalar hair (KBHsSH).

**Key words.** black hole physics

Use \titlerunning to supply a shorter title and/or \authorrunning to supply a shorter list of authors.

## 1. Introduction

### 2. Framework

We use the stationary and axisymmetric metric ansatz provided by Herdeiro & Radu (2014)

$$ds^2 = e^{2F_1} \left( \frac{dr^2}{N} + r^2 d\theta^2 \right) + e^{2F_2} r^2 \sin^2 \theta (d\phi - W dt)^2 - e^{2F_0} N dt^2, \quad (1)$$

with  $N = 1 - r_H/r$ , where  $r_H$  is the radius of the event horizon of the BH and  $W, F_1, F_2, F_0$  are functions of  $r$  and  $\theta$ .

#### 2.1. Distribution of angular momentum and equations of motion

We consider a constant angular momentum distribution  $l(r, \theta) = \text{cte.}$ . The specific value of the angular momentum is computed as the minimum of the following equation

$$I_b^\pm(r, \theta) = \frac{g_{t\phi} \pm \left( \sqrt{g_{t\phi}^2 - g_{tt}g_{\phi\phi}} \right) \sqrt{1 + g_{tt}}}{-g_{tt}} \quad (2)$$

where the plus sign is for prograde orbits and the minus is for retrograde orbits. This expression is given by (Daigne & Font 2004) for Kerr BHs, but it is valid for any stationary, axisymmetric spacetimes. For prograde motion, the function has a minimum outside the event horizon. The location of said minimum corresponds with the marginally bound orbit  $r_{mb}$ , and the angular momentum corresponds to the keplerian angular momentum at that point. This choice of angular momentum distributions is motivated by its simplicity (for a first study of thick tori around KBHsSH) and for allowing the presence of a cusp (this allows matter accretion onto the black hole) and a centre.

#### 2.2. Magnetized disks

We use the procedure described by Montero et al. (2007), where we write the equations of ideal general relativistic MHD are the following conservation laws,  $\nabla_\mu T^{\mu\nu} = 0$ ,  $\nabla_\mu {}^*F^{\mu\nu} = 0$ , and  $\nabla_\mu (\rho u^\mu) = 0$ , where  $\nabla_\mu$  is the covariant derivative and

$$T^{\mu\nu} = (\rho h + b^2)u^\mu u^\nu + \left( p + \frac{1}{2}b^2 \right)g^{\mu\nu} - b^\mu b^\nu, \quad (3)$$

is the energy-momentum tensor of a magnetised perfect fluid,  $h$ ,  $\rho$   $p$  being the fluid specific enthalpy, density and fluid pressure, respectively. Moreover,  ${}^*F^{\mu\nu} = b^\mu u^\nu - b^\nu u^\mu$  is the (dual of the) Faraday tensor relative to an observer with four-velocity  $u^\mu$ , and  $b^\mu$  is the magnetic field in that frame, with  $b^2 = b^\mu b_\mu$ . Assuming the magnetic field is purely azimuthal, i.e.  $b^r = b^\theta = 0$ , and taking into account that the flow is stationary and axisymmetric, the conservation of the current density and of the Faraday tensor follow. Contracting the divergence of Eq. (3) with the projection tensor  $h^\alpha_\beta = \delta^\alpha_\beta + u^\alpha u_\beta$ , we arrive at

$$(\rho h + b^2)u_\nu \partial_i u^\nu + \partial_i \left( p + \frac{b^2}{2} \right) - b_\nu \partial_i b^\nu = 0, \quad (4)$$

where  $i = r, \theta$ . Then, we rewrite this equation in terms of the specific angular momentum  $l$  and of the angular velocity  $\Omega$ , to obtain

$$\partial_i (\ln u_t) - \frac{\Omega \partial_i l}{1 - l\Omega} + \frac{\partial_i p}{w} + \frac{\partial_i (\mathcal{L}b^2)}{2\mathcal{L}w} = 0, \quad (5)$$

where  $\mathcal{L} = g_{t\phi}^2 - g_{tt}g_{\phi\phi}$ . To integrate Eq. (5) we first assume a polytropic equation of state of the form

$$p = K\rho^\Gamma, \quad (6)$$

with  $K$  and  $\Gamma$  constants. Then, we define the magnetic pressure as  $p_m = b^2/2$ , and introduce the definitions  $\tilde{p}_m = \mathcal{L}p_m$  and

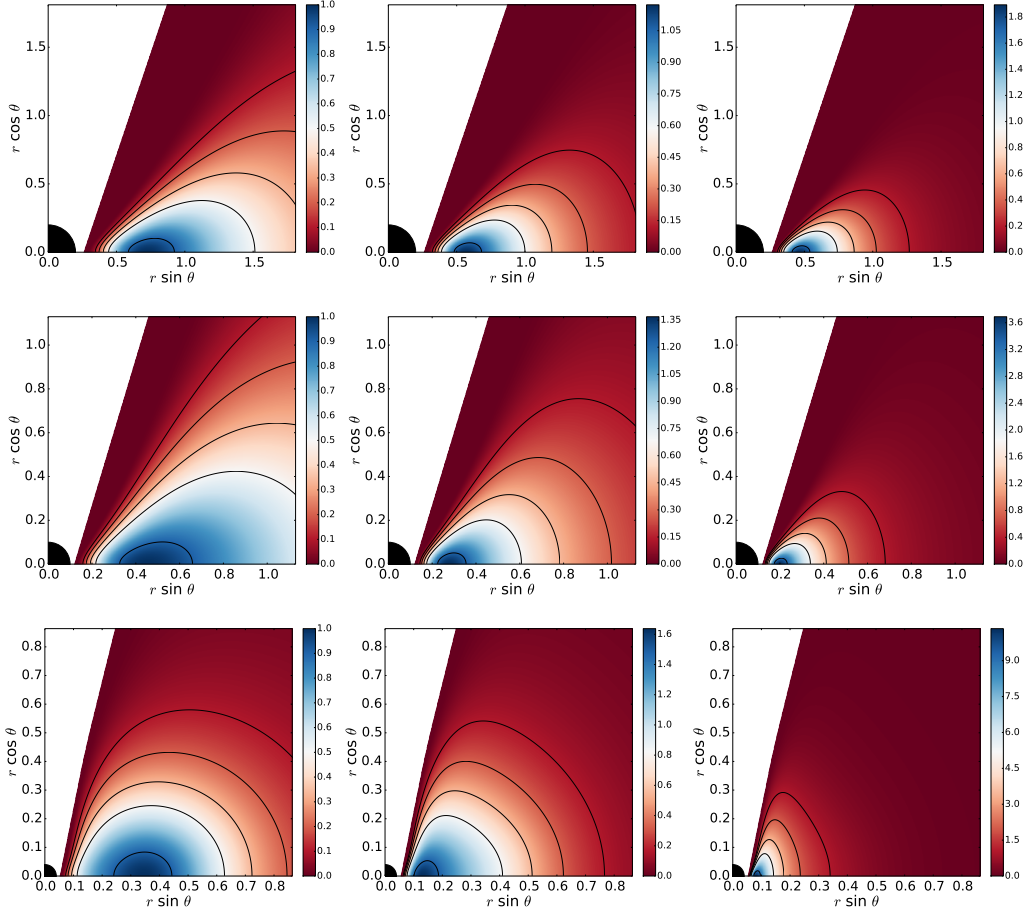


**Fig. 1.** Rest-mass density distribution. From top to bottom the rows correspond to the different models for the KBHsSH (I, II and III). From left to right the columns correspond to different values of the magnetization parameter, namely non-magnetized ( $\beta_{mc} = 10^3$ ), mildly magnetized ( $\beta_{mc} = 1$ ) and strongly magnetized ( $\beta_{mc} = 10^{-3}$ )

$\tilde{w} = \mathcal{L}w$ , in order to write an analogue equation to Eq. (6) for  $\tilde{p}_m$  (Komissarov 2006)

$$\tilde{p}_m = M\tilde{w}^q, \quad (7)$$

or, in terms of the magnetic pressure  $p_m$

$$p_m = M\mathcal{L}^{q-1}w^q, \quad (8)$$

where  $w = \rho h$  is the fluid enthalpy density, and  $M$  and  $q$  are constants. If we define the potential as  $W \equiv \ln|u_t|$ , then we can integrate the equation (5) as

$$W - W_{in} + \ln\left(1 + \frac{\Gamma K}{\Gamma + 1}\rho^{\gamma-1}\right) + \frac{q}{q-1}M(\mathcal{L}w)^{q-1} = 0, \quad (9)$$

where  $W_{in}$  is the potential at the inner edge of the disk.

In this work, we use  $q = \Gamma = 4/3$ , the density at the disk centre  $\rho_c = 1$  and the angular momentum distribution gives us  $W_{in} = 0$ . With this information we can compute all the relevant physical quantities.

It is relevant to note that we could have used the framework described by Komissarov (2006). As we will show in appendix A, we do not take this approach because it is not appropriate for some cases of KBHsSH.

**Table 1.** List of models of KBHsSH.

	$M_{ADM}$	$J_{ADM}$	$M_H$	$J_H$	$M_{SF}$	$J_{SF}$	$r_H$
I	0.415	0.172	0.393	0.15	0.022	0.022	0.2
II	0.933	0.739	0.234	0.114	0.699	0.625	0.1
III	0.975	0.85	0.018	0.002	0.957	0.848	0.04

### 3. Method

#### 3.1. Building the disk

#### 3.2. Numerical method

### 4. Results

It is easy to note the differences between the cases with scalar hair and their KBH counterparts, specially the disk size, shape and physical magnitudes.

### 5. Conclusions

Our results show significant differences between KBHsSH and their counterpart KBH with the same ADM quantities and we think it is worth to expand these results with more KBHsSH cases.

*Acknowledgements.*

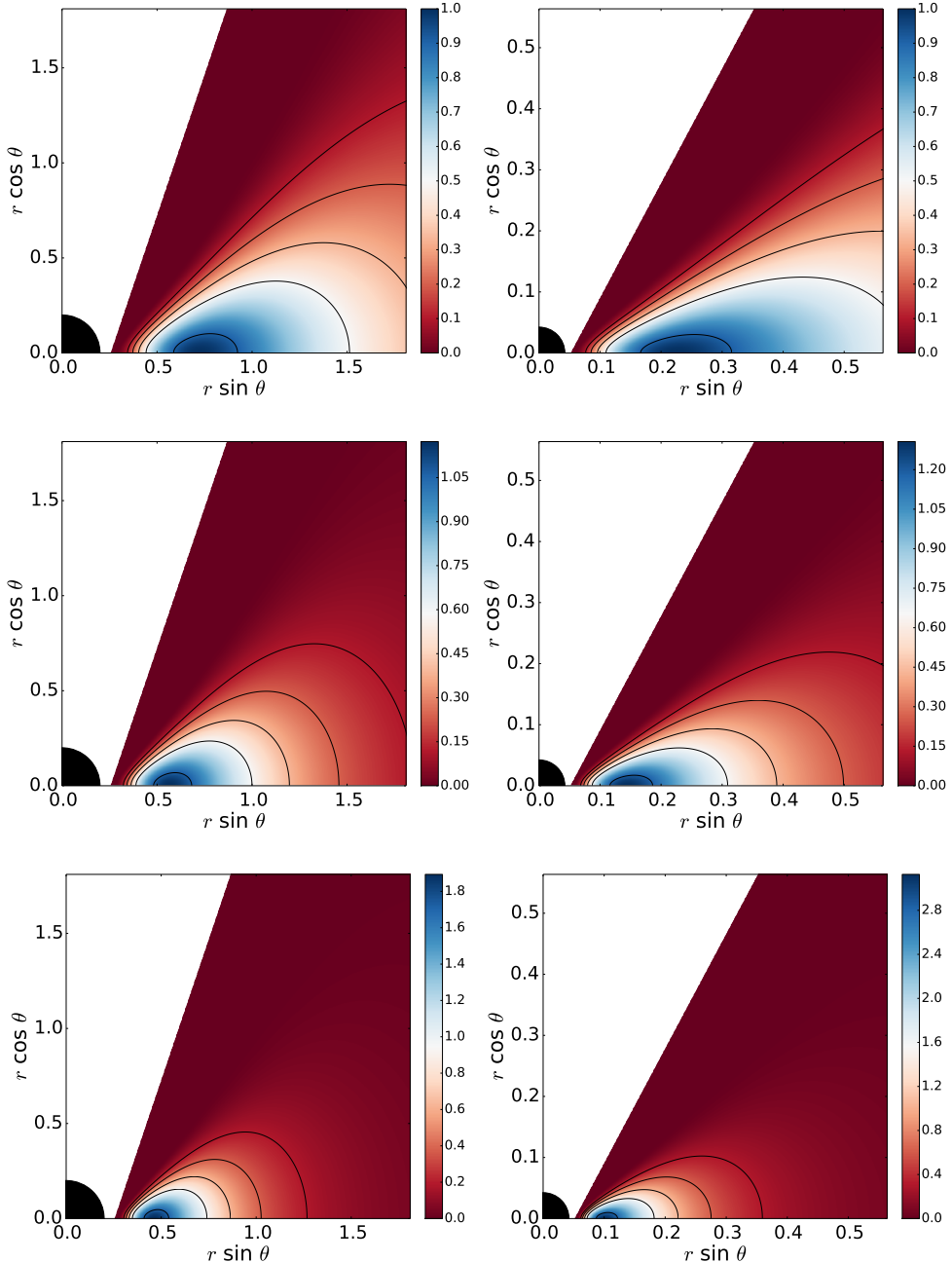


**Fig. 2.** Rest-mass density distribution for the model I. From top to bottom the rows correspond to the different values of the magnetization parameter, namely non-magnetized ( $\beta_{mc} = 10^3$ ), mildly magnetized ( $\beta_{mc} = 1$ ) and strongly magnetized ( $\beta_{mc} = 10^{-3}$ ). The left column correspond to the KBHsSH model and the right column correspond to the corresponding KBH with the same ADM quantities.

## References

- Abramowicz, M., Jaroszynski, M., & Sikora, M. 1978, A&A, 63, 221
- Daigne, F. & Font, J. A. 2004, MNRAS, 349, 841
- Herdeiro, C. A. R. & Radu, E. 2014, Physical Review Letters, 112, 221101
- Komissarov, S. S. 2006, MNRAS, 368, 993
- Montero, P. J., Zanotti, O., Font, J. A., & Rezzolla, L. 2007, MNRAS, 378, 1101

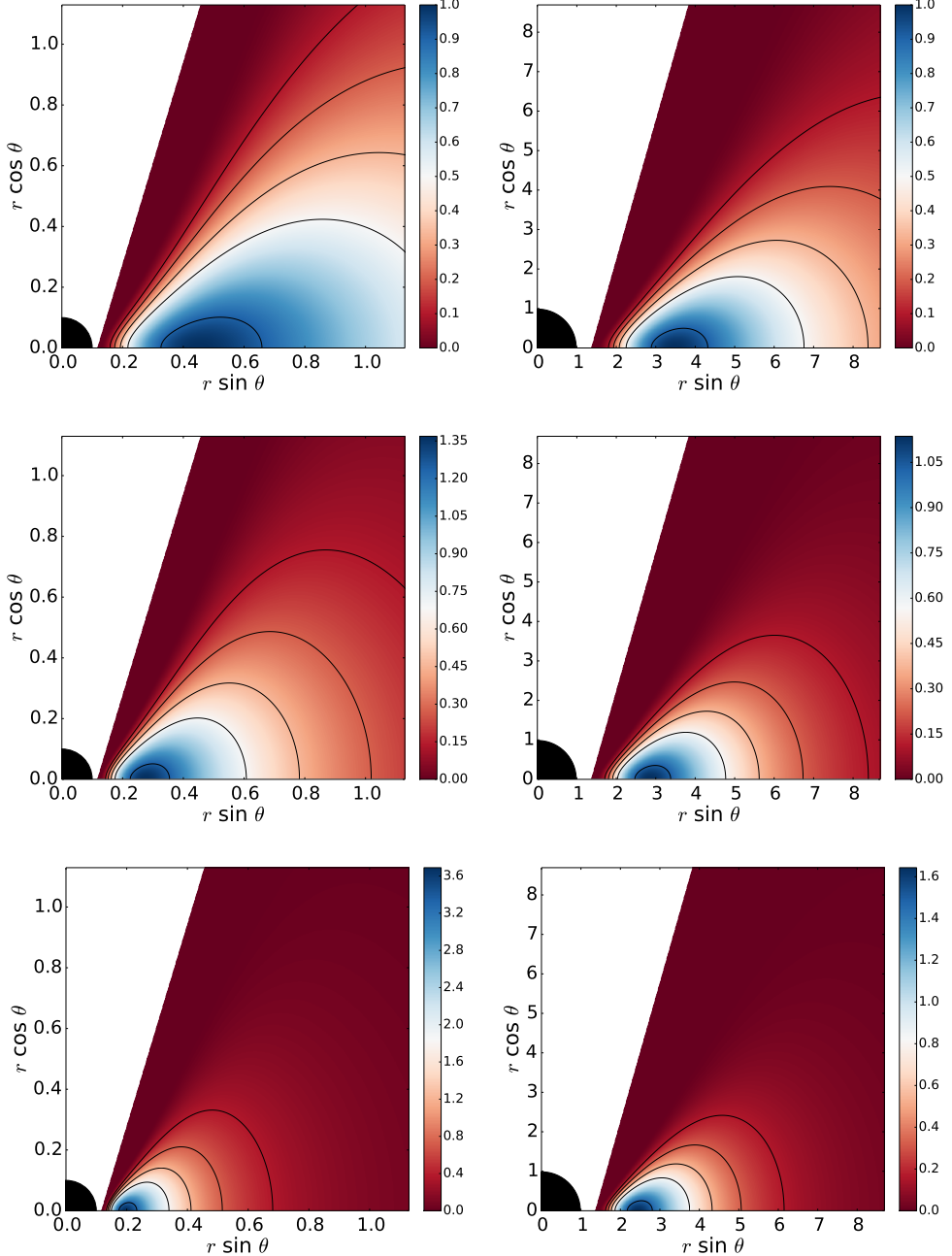


**Fig. 3.** Rest-mass density distribution for the model II. From top to bottom the rows correspond to the different values of the magnetization parameter, namely non-magnetized ( $\beta_{mc} = 10^3$ ), mildly magnetized ( $\beta_{mc} = 1$ ) and strongly magnetized ( $\beta_{mc} = 10^{-3}$ ). The left column correspond to the KBHsSH model and the right column correspond to the corresponding KBH with the same ADM quantities.

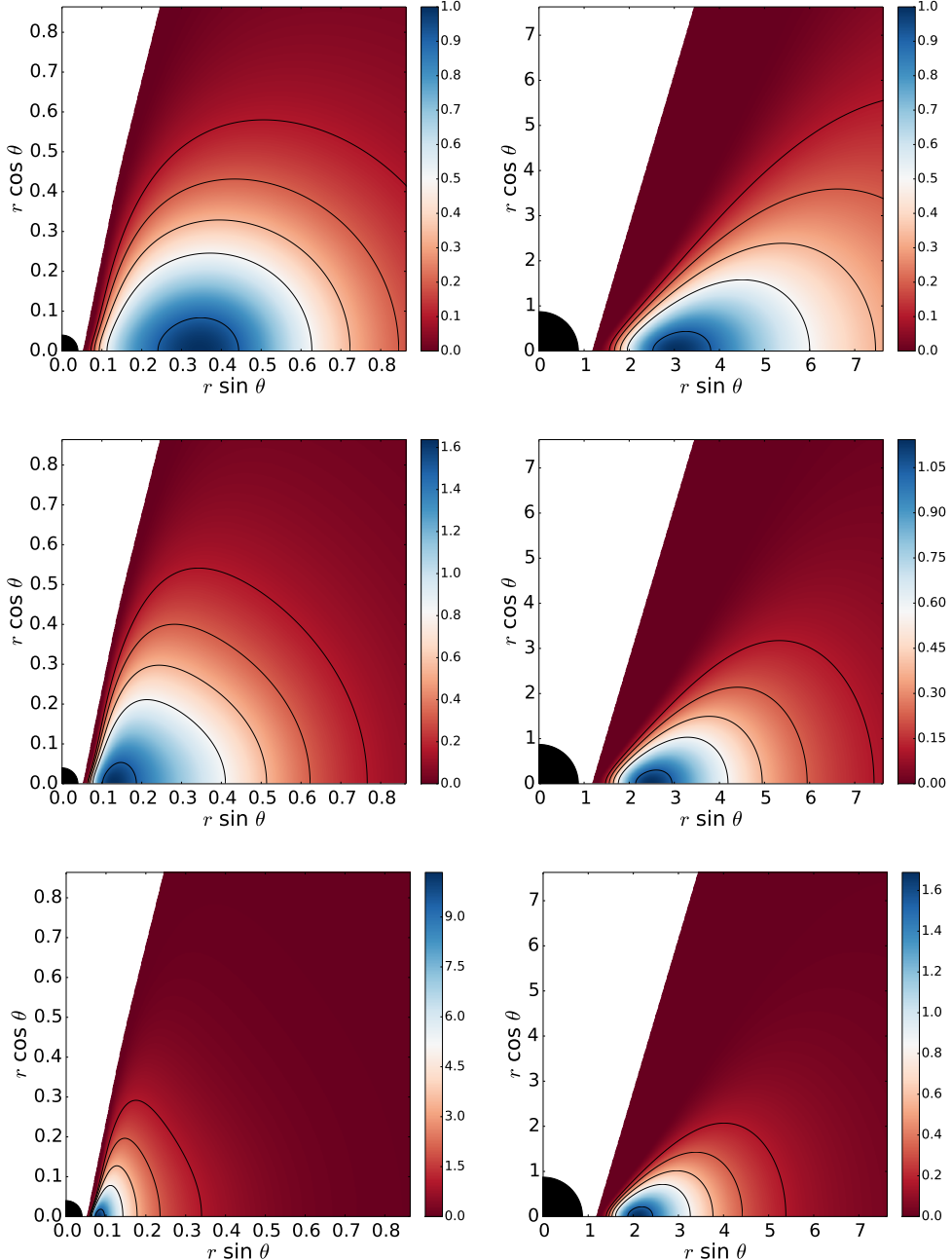


**Fig. 4.** Rest-mass density distribution for the model III. From top to bottom the rows correspond to the different values of the magnetization parameter, namely non-magnetized ( $\beta_{mc} = 10^3$ ), mildly magnetized ( $\beta_{mc} = 1$ ) and strongly magnetized ( $\beta_{mc} = 10^{-3}$ ). The left column correspond to the KBHsSH model and the right column correspond to the corresponding KBH with the same ADM quantities.

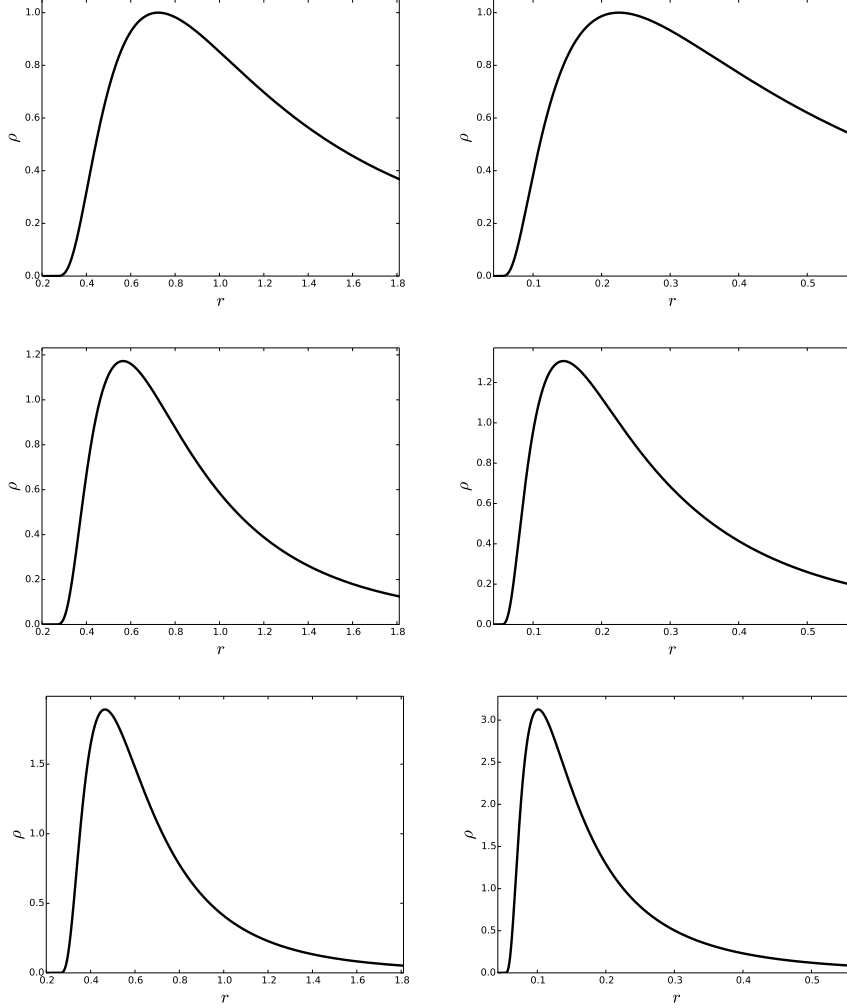


**Fig. 5.** Radial rest-mass density distribution for the model I at the equatorial plane. From top to bottom the rows correspond to the different values of the magnetization parameter, namely non-magnetized ( $\beta_{m\bar{c}} = 10^3$ ), mildly magnetized ( $\beta_{m\bar{c}} = 1$ ) and strongly magnetized ( $\beta_{m\bar{c}} = 10^{-3}$ ). The left column correspond to the KBHsSH model and the right column correspond to the corresponding KBH with the same ADM quantities.

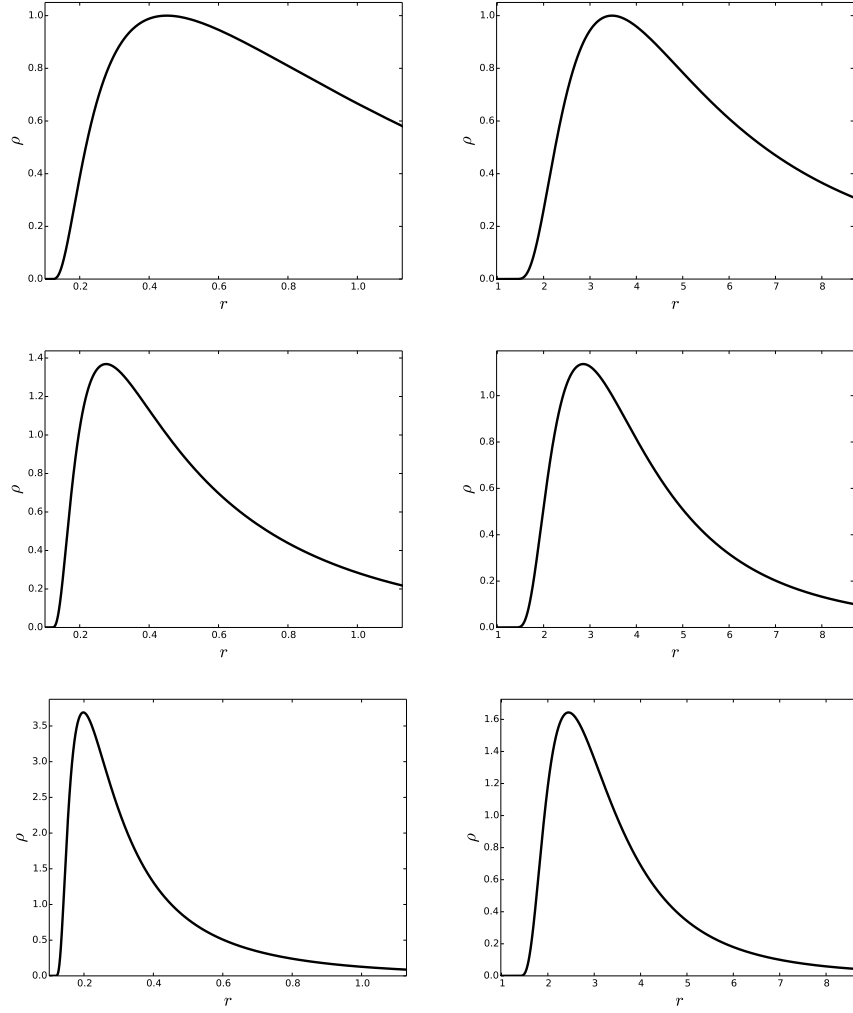


**Fig. 6.** Radial rest-mass density distribution for the model II at the equatorial plane. From top to bottom the rows correspond to the different values of the magnetization parameter, namely non-magnetized ( $\beta_{m_c} = 10^3$ ), mildly magnetized ( $\beta_{m_c} = 1$ ) and strongly magnetized ( $\beta_{m_c} = 10^{-3}$ ). The left column correspond to the KBHsSH model and the right column correspond to the corresponding KBH with the same ADM quantities.

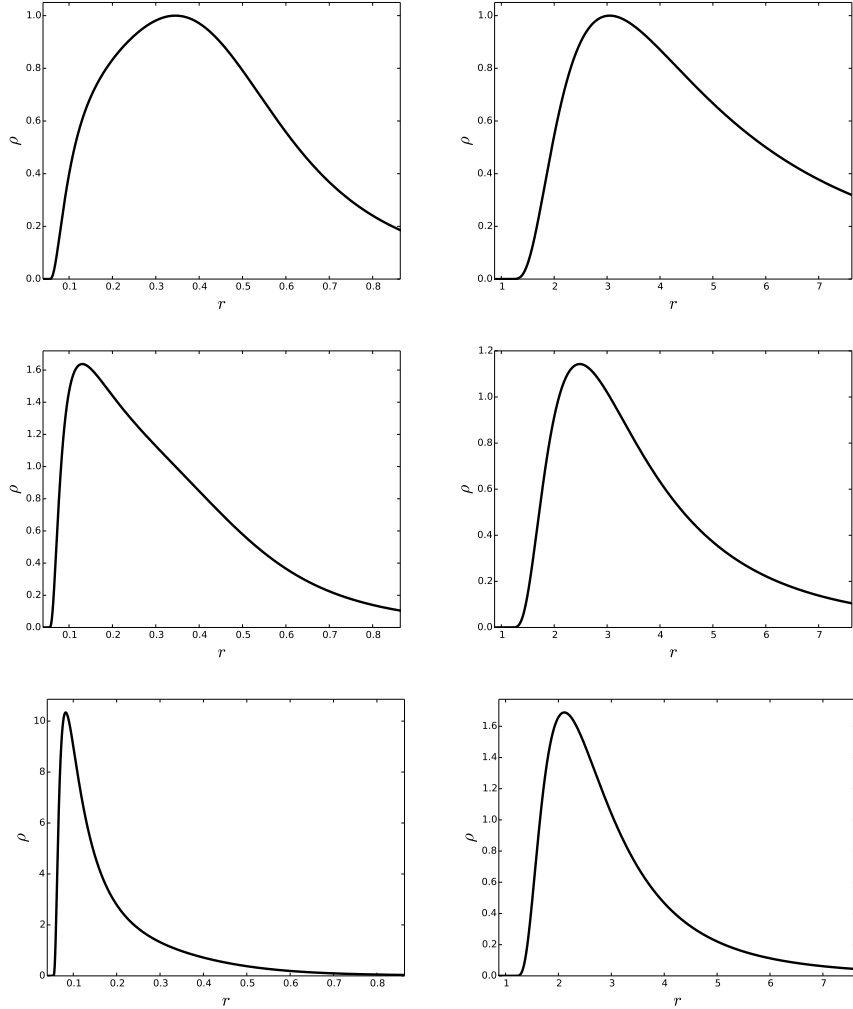


**Fig. 7.** Radial rest-mass density distribution for the model III at the equatorial plane. From top to bottom the rows correspond to the different values of the magnetization parameter, namely non-magnetized ( $\beta_{m_c} = 10^3$ ), mildly magnetized ( $\beta_{m_c} = 1$ ) and strongly magnetized ( $\beta_{m_c} = 10^{-3}$ ). The left column correspond to the KBHsSH model and the right column correspond to the corresponding KBH with the same ADM quantities.

**Table A.1.** Potential at the center  $W_c$  and specific enthalpy at the center  $h_c$  for the non-magnetized case for the three models.

	I	II	III
$W_c$	-0.188	-0.547	-1.236
$h_c$	1.21	1.73	3.44

## Appendix A: KBHsSH vs $h = 1$ approximation

In the figures A.1, A.2, A.3, A.4, A.5, A.6 we show the comparison between the results for KBHsSH using Montero et al. (2007) and Komissarov (2006). The figures show good agreement for the highly magnetized case ( $\beta_{m_c} = 10^{-3}$ ) but not quite for the non-magnetized and mildly magnetized cases, especially for the model III. This is due to the  $h = 1$  approximation breaking down. In the table A.1 we show the correlation between the value of the potential at the centre and the specific enthalpy at the centre. It is easy to note that for higher absolute values of  $W_c$  we get values of  $h_c$  further away from the case  $h = 1$ . This is interesting because these high values of  $W_c$  (particularly the one for the model III) is unattainable for any KBH (as is shown by Abramowicz et al. (1978), the maximum value of  $W_c$  for a KBH is  $W_c = 0.549$ ).

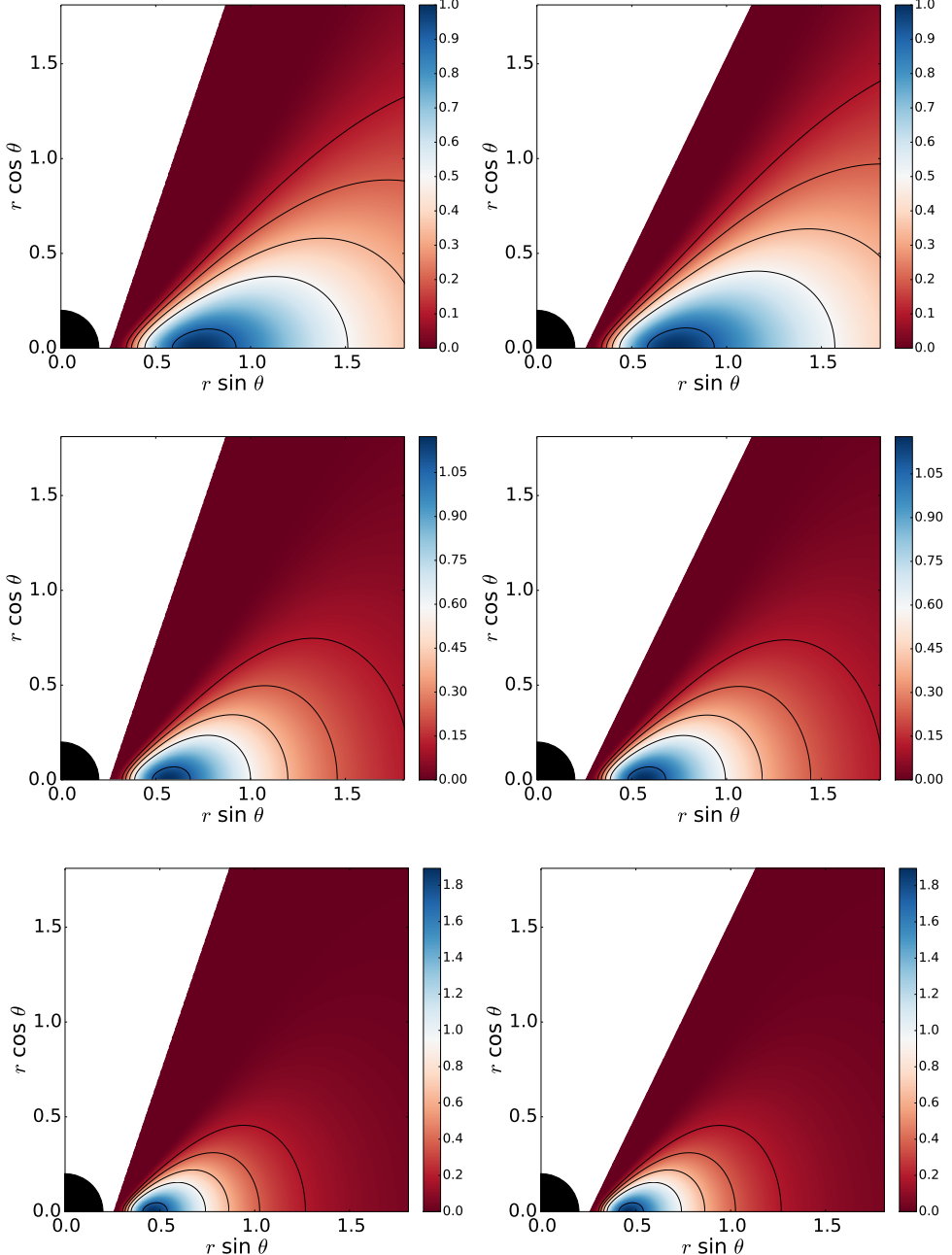


**Fig. A.1.** Rest-mass density distribution for the model I. From top to bottom the rows correspond to the different values of the magnetization parameter, namely non-magnetized ( $\beta_{mc} = 10^3$ ), mildly magnetized ( $\beta_{mc} = 1$ ) and strongly magnetized ( $\beta_{mc} = 10^{-3}$ ). The left column correspond to the KBHsSH model using Montero et al. (2007) and the right column correspond to the Komissarov (2006) approximation.

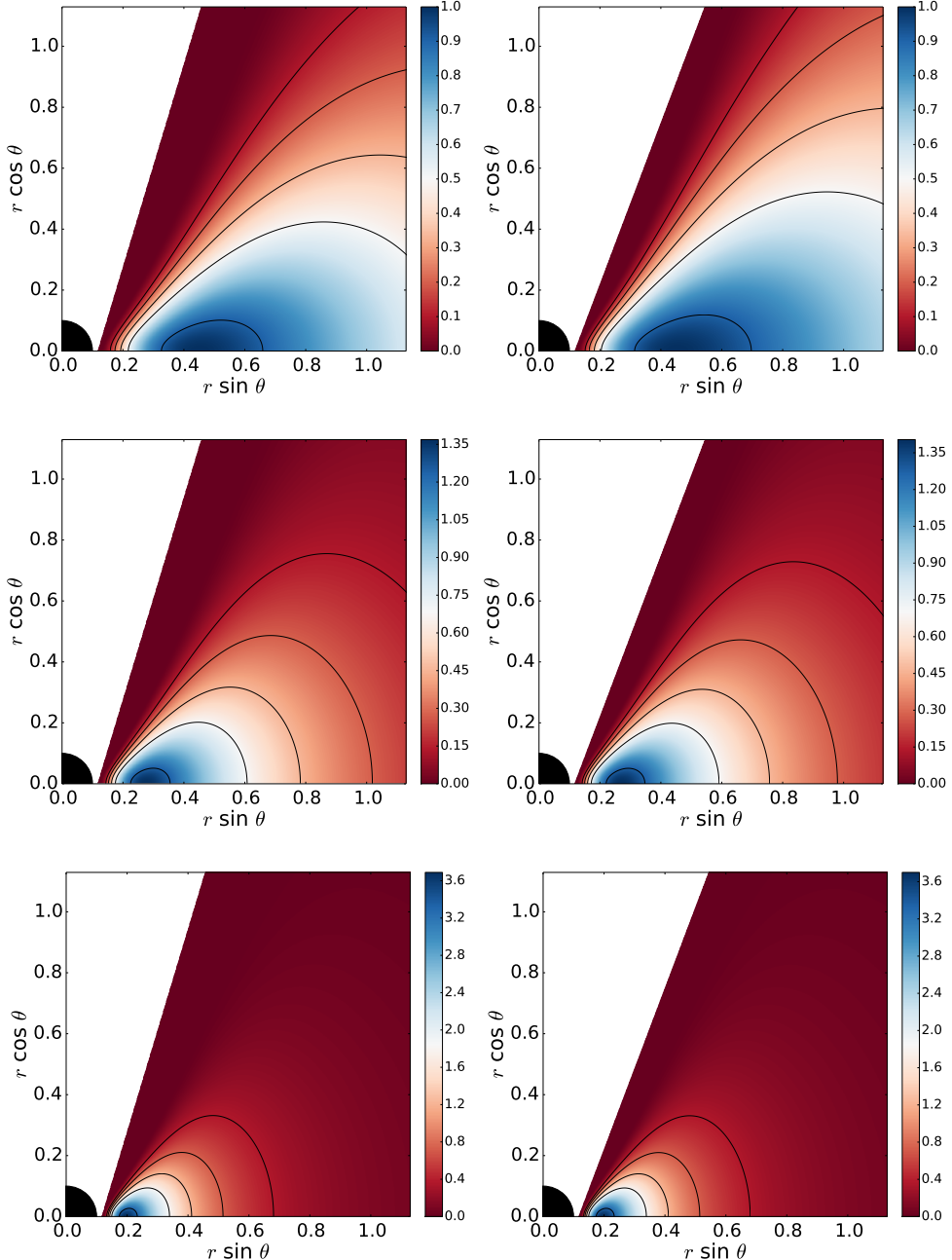


**Fig. A.2.** Rest-mass density distribution for the model II. From top to bottom the rows correspond to the different values of the magnetization parameter, namely non-magnetized ( $\beta_{mc} = 10^3$ ), mildly magnetized ( $\beta_{mc} = 1$ ) and strongly magnetized ( $\beta_{mc} = 10^{-3}$ ). The left column correspond to the KBHsSH model using Montero et al. (2007) and the right column correspond to the Komissarov (2006) approximation.

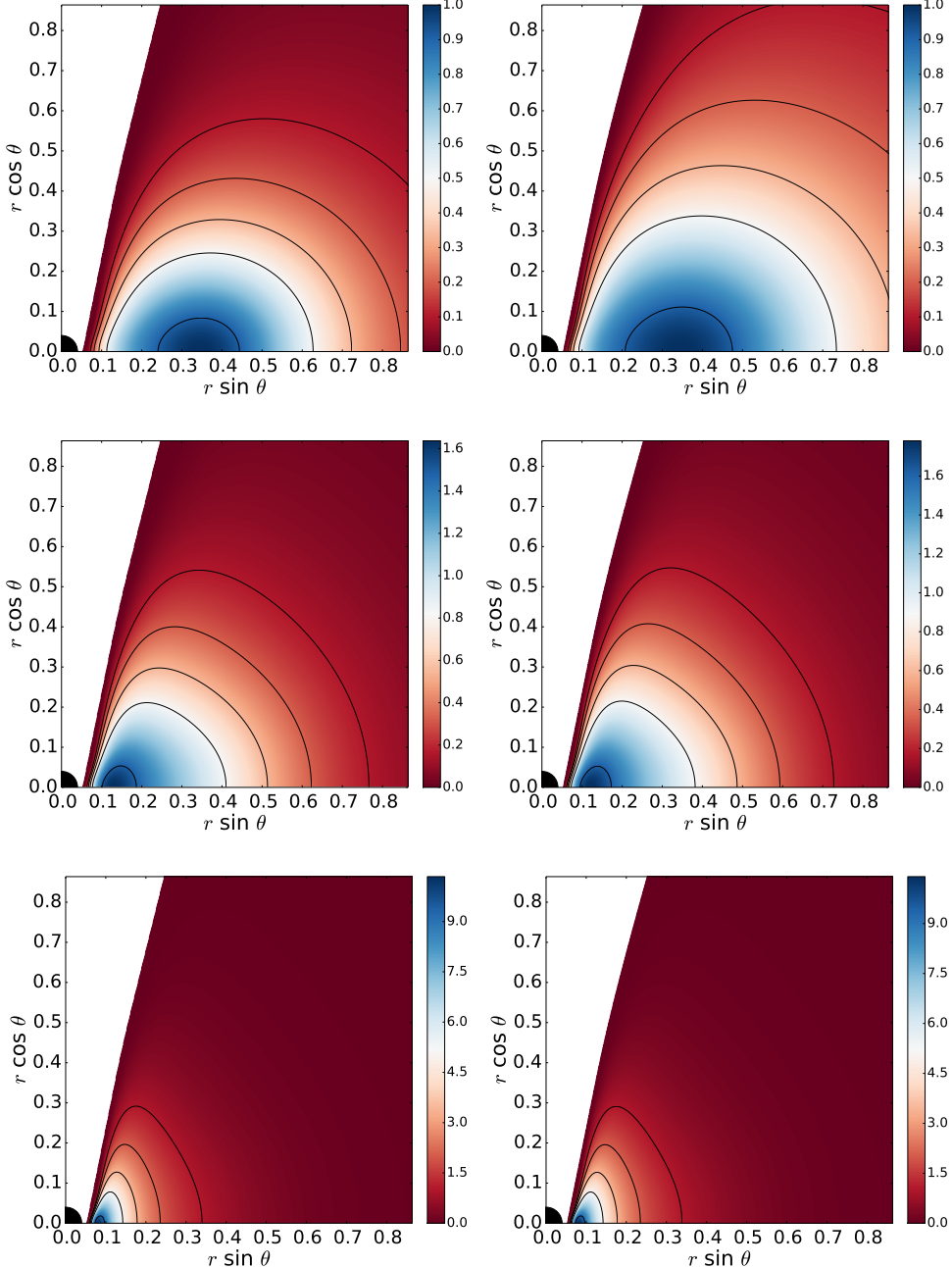


**Fig. A.3.** Rest-mass density distribution for the model III. From top to bottom the rows correspond to the different values of the magnetization parameter, namely non-magnetized ( $\beta_{mc} = 10^3$ ), mildly magnetized ( $\beta_{mc} = 1$ ) and strongly magnetized ( $\beta_{mc} = 10^{-3}$ ). The left column correspond to the KBHsSH model using Montero et al. (2007) and the right column correspond to the Komissarov (2006) approximation.

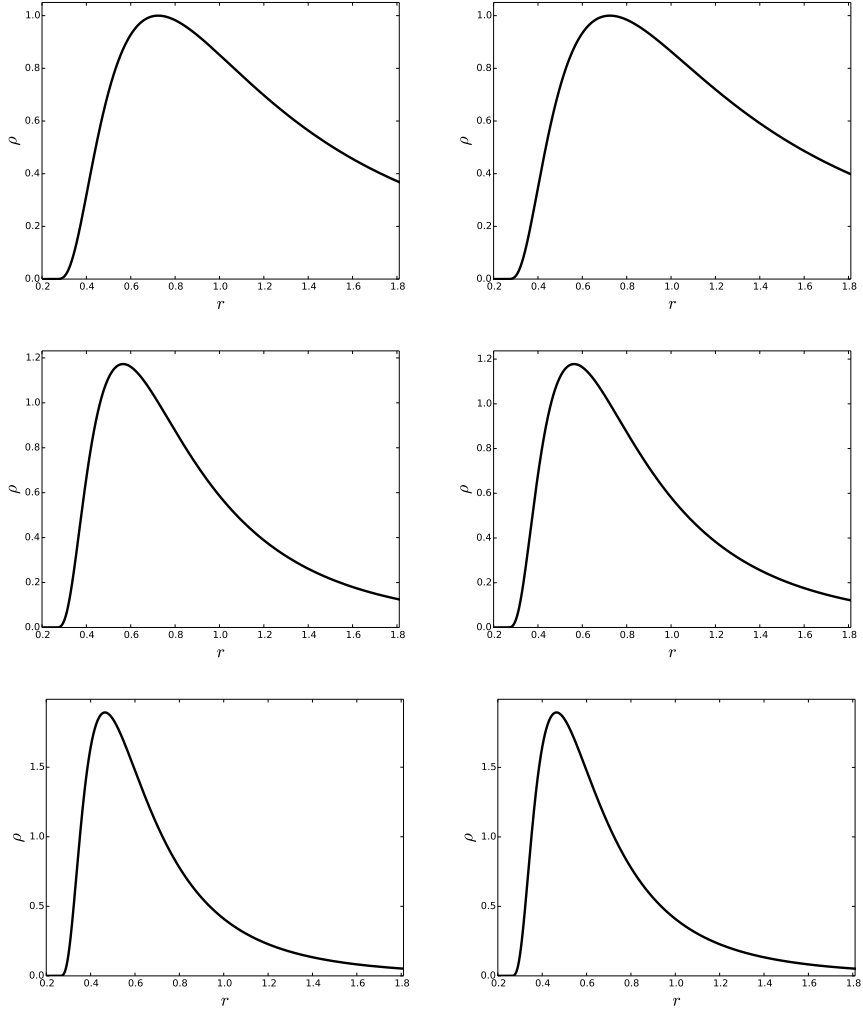


**Fig. A.4.** Radial rest-mass density distribution for the model I at the equatorial plane. From top to bottom the rows correspond to the different values of the magnetization parameter, namely non-magnetized ( $\beta_{m_c} = 10^3$ ), mildly magnetized ( $\beta_{m_c} = 1$ ) and strongly magnetized ( $\beta_{m_c} = 10^{-3}$ ). The left column correspond to the KBHsSH model using Montero et al. (2007) and the right column correspond to the Komissarov (2006) approximation.

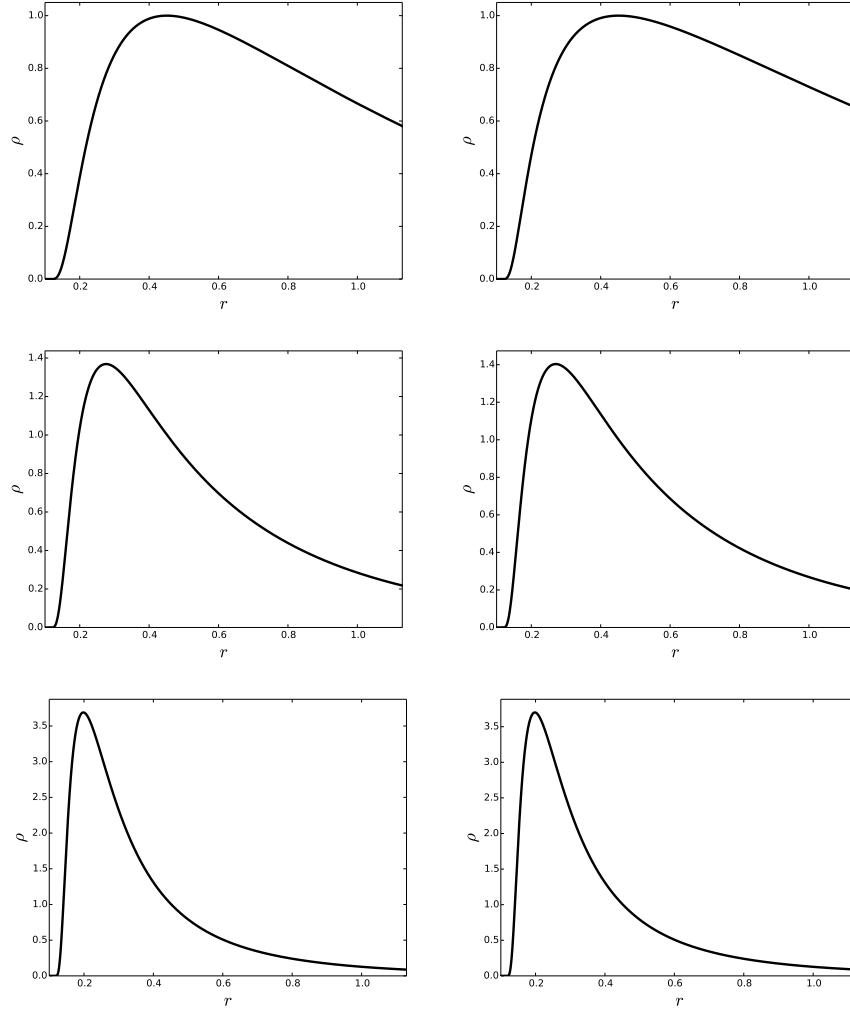


**Fig. A.5.** Radial rest-mass density distribution for the model II at the equatorial plane. From top to bottom the rows correspond to the different values of the magnetization parameter, namely non-magnetized ( $\beta_{m_c} = 10^3$ ), mildly magnetized ( $\beta_{m_c} = 1$ ) and strongly magnetized ( $\beta_{m_c} = 10^{-3}$ ). The left column correspond to the KBHsSH model using Montero et al. (2007) and the right column correspond to the Komissarov (2006) approximation.

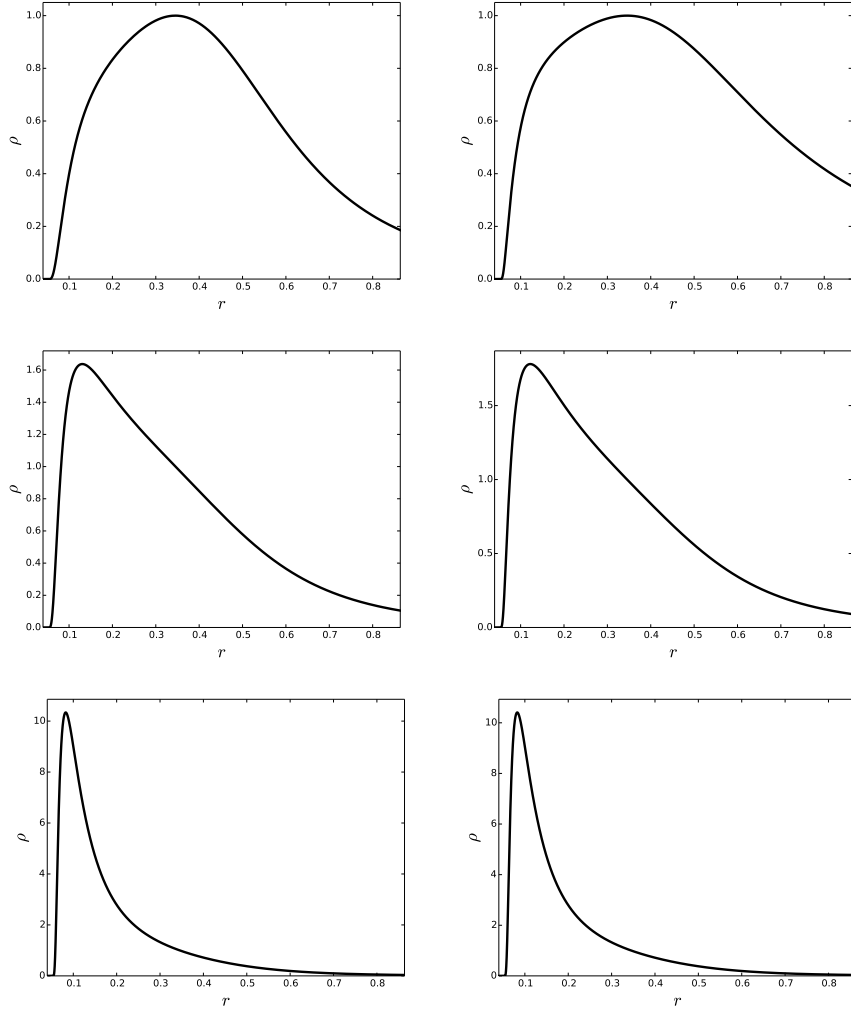


**Fig. A.6.** Radial rest-mass density distribution for the model III at the equatorial plane. From top to bottom the rows correspond to the different values of the magnetization parameter, namely non-magnetized ( $\beta_{m_c} = 10^3$ ), mildly magnetized ( $\beta_{m_c} = 1$ ) and strongly magnetized ( $\beta_{m_c} = 10^{-3}$ ). The left column correspond to the KBHsSH model using Montero et al. (2007) and the right column correspond to the Komissarov (2006) approximation.